Journal of Power Sources 220 (2012) 74–78

Contents lists available at SciVerse ScienceDirect

Journal of Power Sources

journal homepage: www.elsevier.com/locate/jpowsour

# Impact of direct butane microtubular solid oxide fuel cells

Hirofumi Sumi*, Toshiaki Yamaguchi, Koichi Hamamoto, Toshio Suzuki, Yoshinobu Fujishiro

*Advanced Manufacturing Research Institute, National Institute of Advanced Industrial Science and Technology, 2266-98 Anagahora, Simo-shidami, Nagoya 463-8560, Japan*

## HIGHLIGHTS

- Rapid degradation occurred for SOFCs with Ni–zirconia anodes in butane.
- Ni–Gd doped ceria anode did not deteriorate for 24 h in butane at 610 °C.
- Redox of ceria contributes to the suppression of carbon deposition.

## ARTICLE INFO

*Article history:*
Received 2 April 2012
Received in revised form
12 June 2012
Accepted 31 July 2012
Available online 8 August 2012

*Keywords:*
Solid oxide fuel cell (SOFC)
Ni-based anodes
Ceria
Hydrocarbon
Carbon deposition

## ABSTRACT

We investigated direct butane power generation for microtubular solid oxide fuel cells with a diameter of less than 2 mm. Conventional Ni-stabilized zirconia anodes deteriorated rapidly over a period of 3–4 h at 610 °C and a low steam/carbon (S/C) ratio of 0.044 in butane due to a large amount of carbon deposition. For the Ni–Gd doped ceria (Ni–GDC) anode, the power could be generated continuously for more than 24 h at 610 °C and S/C = 0.044 in butane. The rate of carbon deposition for the Ni–GDC was slower than that for the Ni-stabilized zirconia at 610 °C. Ceria can be reduced from $Ce^{4+}$ to $Ce^{3+}$, which causes the suppression of carbon deposition on the Ni–GDC anode in butane at low humidity.



## 1. Introduction

Solid oxide fuel cells (SOFCs) can, in principle, directly use not only hydrogen but also hydrocarbon fuels such as methane, propane, butane and so on. However, hydrocarbon is decomposed into hydrogen and solid carbon at high temperatures.

$$C_xH_y \rightarrow xC + (y/2)H_2 \quad (1)$$

Carbon deposition causes rapid deterioration due to the deactivation of electrode catalysts and the inhibition of fuel diffusion [1]. Steam reforming of hydrocarbons is generally applied with a steam/carbon (S/C) ratio greater than two in order to prevent carbon deposition.

$$C_xH_y + xH_2O \rightarrow xCO + (x + y/2)H_2 \quad (2)$$

It is desirable to reduce the S/C ratio because the introduction of an excess amount of water causes a decrease in power generation efficiency and complicates the water supply systems. For methane fuel, power generation with internal reforming has been demonstrated at an S/C ratio of only 0.03 through the use of a Ni–Sc stabilized zirconia (Ni–ScSZ) anode [2] or by decreasing the operating temperature to 550–650 °C for SOFCs [3]. Methane is the main component of natural gas, which is a suitable fuel for stationary applications. The effects of $O^{2-}$ ionic conductors in the anode on the carbon deposition behavior were investigated for methane fuel. It was reported that the rate of the carbon deposition adheres to the following sequence in methane at 1000 °C: Ni–Sm doped ceria (Ni–SDC) > Ni–Y stabilized zirconia (Ni–YSZ) > Ni–ScSZ [4]. The performance of Cu–YSZ anode with ceria was higher than that without ceria in dry methane [5]. The graphitization degree varied with respect to the change in oxide species and the operating temperature in methane, which strongly affected the durability against the carbon deposition [6–8].

On the other hand, fuels such as propane, butane and so on are suitable for portable applications due to the fact that they can be liquefied easily. However, it is well known that carbon is easier to be deposited, when the carbon number in hydrocarbon fuels increases [9,10]. Gorte et al. demonstrated direct butane power generation for SOFCs using a Cu–ceria anode [11]. Although the Cu-

* Corresponding author. Tel.: +81 52 736 7592; fax: +81 52 736 7405.
*E-mail address:* h-sumi@aist.go.jp (H. Sumi).

0378-7753/$ – see front matter © 2012 Elsevier B.V. All rights reserved.
http://dx.doi.org/10.1016/j.jpowsour.2012.07.106

based anodes can inhibit carbon deposition in comparison to Ni-based anodes, the Cu-based anodes have a lower catalytic activity of electrochemical fuel oxidation. It was reported that a bi-metallic Cu–Co-based anode was expected to show high performance in dry *n*-butane [12]. Ceramic anodes such as $La_4Sr_{n-4}Ti_nO_{3n+2}$ were also investigated for power generation with internal reforming of hydrocarbon fuels [13]. Several researchers tried direct utilization of hydrocarbon fuels such as methanol [14,15], ethanol [16,17], propane [18,19], *n*-butane [20–22], *n*-decane [23], *n*-dodecane [24], toluene [25], biogas [26] and so on in SOFCs. However, it is insufficient to investigate the $O^{2-}$ ionic conductors such as zirconia and ceria in an anode when the goal is to improve the durability against the carbon deposition in the heavy hydrocarbon fuels.

Lowering the operating temperature significantly contributes to a decrease in the rate of carbon deposition for SOFCs. Kendall et al. [27,28] and Yashiro et al. [29] demonstrated direct butane power generation for a short time using microtubular SOFCs. The compatibility of a low operating temperature (550 °C) and a high power density (1 W $cm^{-2}$) were verified for microtubular cells with microstructural controlled anodes in hydrogen fuel [30,31]. If direct butane power generation is stable for these Ni-based anode-supported microtubular SOFCs, it is also expected that a highly efficient portable power source can be realized. Fuel and water supply systems are supposed to be simplified to reduce the costs for small portable power sources. Therefore, no deterioration of the anode performance is expected to occur, even if dry butane fuel is supplied in an emergency situation. In this study, we demonstrated direct butane power generation for microtubular SOFCs with microstructural controlled Ni–$O^{2-}$ ionic conductor composite anodes.

## 2. Experimental

We chose the conventional oxides of 8 mol% Y-stabilized zirconia (YSZ; Tosoh), 10 mol% Sc and 1 mol% Ce-stabilized zirconia (ScSZ; Daiichi Kigenso Kagaku Kogyo), and 10 mol% Gd-doped ceria (GDC; Shin-Etsu Chemical) for the $O^{2-}$ ionic conductors in the anodes. The weight ratio of NiO (Sumitomo metal mining) to these oxides was 6:4. A pore former of acrylic resin with a grain size of *ca.* 5 μm (Sekisui Plastic) was added before sintering to increase anode porosity. The porosity after reduction was *ca.* 40 vol.%. The YSZ and 70 wt.% $La_{0.6}Sr_{0.4}Co_{0.2}Fe_{0.8}O_3$ (LSCF; Dowa Electronics Materials)-GDC were used as the electrolyte and cathode materials, respectively. The GDC interlayer was introduced between the electrolyte and the cathode to prevent chemical reactions with these materials. The thickness of anode, electrolyte, interlayer and cathode were 200, 5, 1 and 20 μm, respectively. The tube diameter and cathode area were 1.8 mm and 0.6 $cm^2$, respectively. For power generation tests, the different fuels were flowed into the inside of a tube at the rate of 100 mL $min^{-1}$, and air was flowed onto the outside of the same tube at 100 mL $min^{-1}$. The operating temperature was 610 °C and a silver wire was used as a current-collector. Details of the sample preparation and characterization are presented in Ref. [32]. The fuel compositions were $H_2$:$H_2O$:$N_2$ = 57:3:40, $CH_4$:$H_2O$:$N_2$ = 38:3:59 (S/C = 0.079), and *n*-$C_4H_{10}$:*i*-$C_4H_{10}$:$H_2O$:$N_2$ = 11:6:3:80 (S/C = 0.044). Each fuel was humidified at room temperature to define an oxygen partial pressure in the anode. The anode microstructures were observed with a field emission-scanning electron microscope (FE-SEM; JEOL JSM-6330F) after direct butane power generation. The rates of carbon deposition were evaluated by thermogravimetry (TG; Shimadzu TG-8120) in dry and humidified butane (S/C = 0.044) at 610 °C after reduction in 57% $H_2$ for 1 h. The NiO–YSZ, NiO–ScSZ and NiO–GDC microtubes were crushed and sieved to a particle size of 0.85–1.7 mm before being used for TG analyses.

## 3. Results and discussion

Fig. 1 shows the weight changes of the NiO–YSZ, NiO–ScSZ and NiO–GDC powders evaluated by TG in hydrogen and butane at 610 °C. The production of water and carbon dioxide is only $3 \times 10^{-4}$ mol by a discharge of 1 A for actual SOFCs. In this study, the hydrogen and butane were diluted to 57% and 17%, respectively, in consideration of experimental safety. The S/C ratio became 0.044 after the diluted butane flew through water at 25 °C. The S/C ratio is the same condition for the power generation in this study. The NiO–YSZ and NiO–ScSZ powders required more than 1 h to reduce completely. For the NiO–GDC powder, the weight decreased rapidly for an initial 15 min, and then the weight was stable. The theoretical weight decrease is 12% for 60 wt.% NiO-oxide after reduction, assuming that the oxides does not change. The weight decrease was 10% for the NiO–YSZ and NiO–ScSZ after reduction for 1 h. On the other hand, the weight decrease reached 13% for the NiO–GDC, which was larger than the theoretical value. This result supports that a part of ceria was also reduced from $Ce^{4+}$ to $Ce^{3+}$. After the atmosphere changed from hydrogen to butane, the weight increased as a result of carbon deposition. The weight increase rates were found to scale in the following order at 610 °C in butane: Ni–ScSZ > Ni–YSZ > Ni–GDC. Although this order is reversed at temperatures in excess of 1000 °C in methane [4], the same order was previously confirmed at the lower temperature of 850 °C [7]. The rate of carbon deposition may be strongly dependent on the ambient temperature in hydrocarbon. In this study, temperature and hydrocarbon species were different from Refs. [4] and [7]. We will investigate the effects of temperature and hydrocarbon species on the rate of carbon deposition in near future. The weight increase rate was the same in dry and humidified butane for Ni–YSZ and Ni–ScSZ. However, the rate in humidified butane decreased significantly in comparison with that in dry butane for Ni–GDC. This suggests that carbon is oxidized catalytically via the promotion of reduction–oxidation (redox) of ceria in the presence of water [33].

$$C + H_2O \rightarrow CO + H_2 \quad (3)$$

The Ni–GDC is expected not only to inhibit carbon deposition, but also to promote the electrochemical oxidation of deposited

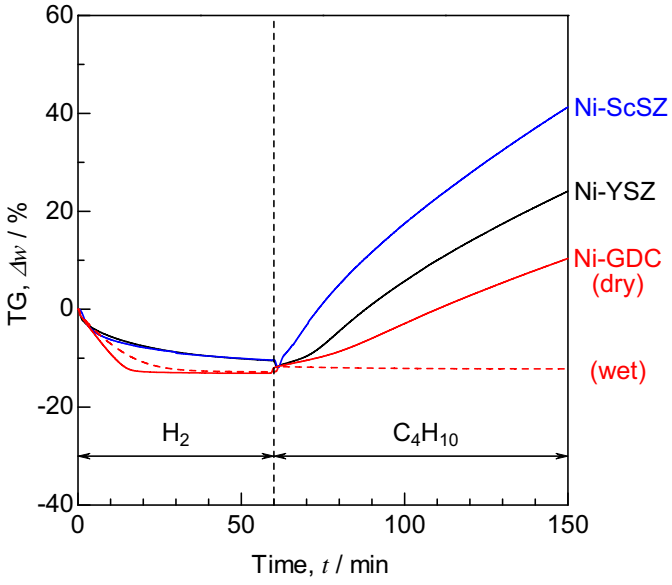


**Fig. 1.** Weight changes of NiO–YSZ, NiO–ScSZ and NiO–GDC powders at 610 °C in $H_2$ and $C_4H_{10}$.

carbon by the production of water during power generation in butane fuel.

Fig. 2 shows the current–voltage ($i$–$V$) and current-power ($i$–$p$) characteristics for the microtubular SOFC with the Ni–GDC anode at 610 °C in hydrogen, methane and butane. The theoretical electromotive forces (EMFs) are 1.12 V in 3% $H_2O$-57% $H_2$, 38% $CH_4$ and 17% $C_4H_{10}$. The open circuit voltage (OCV; $i = 0$) was the same as the EMF in each fuel. A maximum power density of 0.55 W cm$^{-2}$ was obtained for the microtubular SOFCs at temperatures as low as 610 °C in hydrogen. However, the power density decreased by half in methane and butane. The slopes of the $i$–$V$ curves became steeper at low current densities for hydrocarbon fuels because of the carbon deposition on the anode at low S/C ratios. The area specific resistances (ASRs), which were derived from the slope of $i$–$V$ curves near OCV, were 1.0, 4.2 and 5.0 Ω cm$^2$ in hydrogen, methane and butane, respectively. These ASRs agreed well with the resistances evaluated using the AC impedance method. The slopes of the $i$–$V$ curves were more gradual at high current densities in the hydrocarbon fuels. This tendency was especially strong in butane. This might be caused by the promotion of the electrochemical oxidation of deposited carbon and the reforming reaction of hydrocarbon at high current densities.

Fig. 3 shows the time course of cell voltage at a drawn current of 0.2 A cm$^{-2}$ for the cells with the Ni–YSZ, Ni–ScSZ and Ni–GDC anodes at 610 °C in hydrogen, methane and butane. For 30 min sequential flows of hydrogen and methane, the cell performances for each anode were almost the same. The cell voltages dropped by 0.7 V immediately after the fuel changed from methane to butane. The voltages increased to 0.8 V for 1 and 10 min after the change to butane fuel for the cells with the Ni–YSZ and Ni–ScSZ anodes, respectively, because the electric conductivity was improved by the deposition of conductive graphite on the anodes [34]. However, power generation was impossible for the cell with the Ni–YSZ and Ni–ScSZ anodes at 610 °C after 3–4 h into the fuel change from methane to butane. A large amount of deposited carbon caused the deterioration of Ni catalytic activity and the inhibition of fuel diffusion. On the other hand, power can be generated continuously for more than 24 h at 610 °C and S/C = 0.044 in butane for the cell with the Ni–GDC anode, although the performance for the Ni–GDC anode was lower than that for the Ni–YSZ and Ni–ScSZ anodes. The

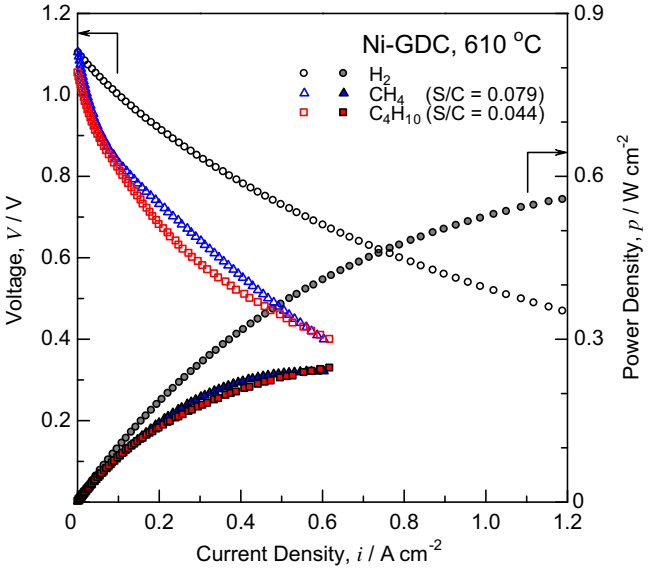


**Fig. 2.** Current–voltage and current–power characteristics for the cells with the Ni–GDC anode at 610 °C in $H_2$ and $C_4H_{10}$.

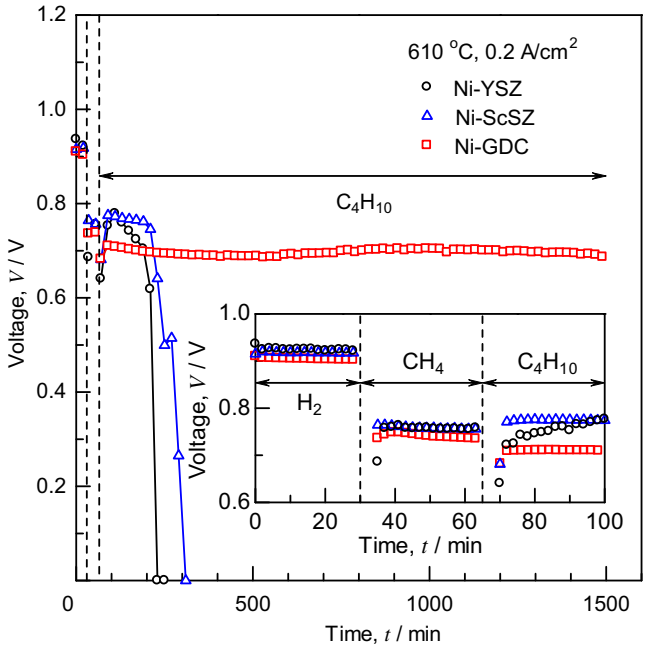


**Fig. 3.** Time course of cell voltage at 0.2 A cm$^{-2}$ for the cells with Ni–YSZ, Ni–ScSZ and Ni–GDC anodes at 610 °C in $H_2$, $CH_4$ and $C_4H_{10}$.

result of thermogravimetry in Fig. 1 indicates the low rate of carbon deposition for the Ni–GDC at 610 °C in butane. Furthermore, the rate was expected to decrease further by the promotion of butane reforming (reaction (2)) and carbon oxidation (reaction (3)) due to the production of water on the anode during power generation.

The microstructures of the Ni–YSZ, Ni–ScSZ and Ni–GDC anodes after power generation at 610 °C in butane for 3, 4 and 24 h, respectively, were observed with FE-SEM as shown in Fig. 4. Carbon was coated on Ni catalysts and carbon nanofibers were grown from the interface between Ni and oxide particles for the Ni–YSZ and Ni–ScSZ anodes after direct butane power generation for 3 and 4 h, respectively. It is well known that the carbon is deposited on the Ni nanoparticles, and it is precipitated in the form of carbon nanofibers under the Ni nanoparticles [35]. The diameter of the carbon nanofibers on the Ni–ScSZ anode was larger than that on the Ni–YSZ anode in comparison with Fig. 4A and B. It was previously confirmed that the size of deposited Ni nanoparticles on ScSZ was larger than that on YSZ after reducing due to the larger change of solid solubility of Ni into ScSZ by redox treatment [8]. The weight increase rate became the largest for the Ni–ScSZ in butane as shown in Fig. 1 because of the growth of the thick carbon nanofibers. In this study, the macropores were formed by adding acrylic resin before sintering. However, the macropores were destroyed in the areas where a large amount of carbon was deposited. For the Ni–GDC anode, the structure of macropores was kept and no carbon nanofiber was observed after direct butane power generation for 24 h. The TG analysis suggests that the rate of deposited carbon was the slowest for Ni–GDC in butane, and a part of the ceria was reduced from $Ce^{4+}$ to $Ce^{3+}$ in hydrogen as shown in Fig. 1. During the butane direct power generation, it is possible for the following reactions to occur by the redox of ceria under carbon deposition conditions.

$$CeO_2 + nC \rightarrow CeO_{2-n} + nCO \quad (4)$$

$$CeO_{2-n} + nH_2O \rightarrow CeO_2 + nH_2 \quad (5)$$

$$CeO_{2-n} + nCO_2 \rightarrow CeO_2 + nCO \quad (6)$$

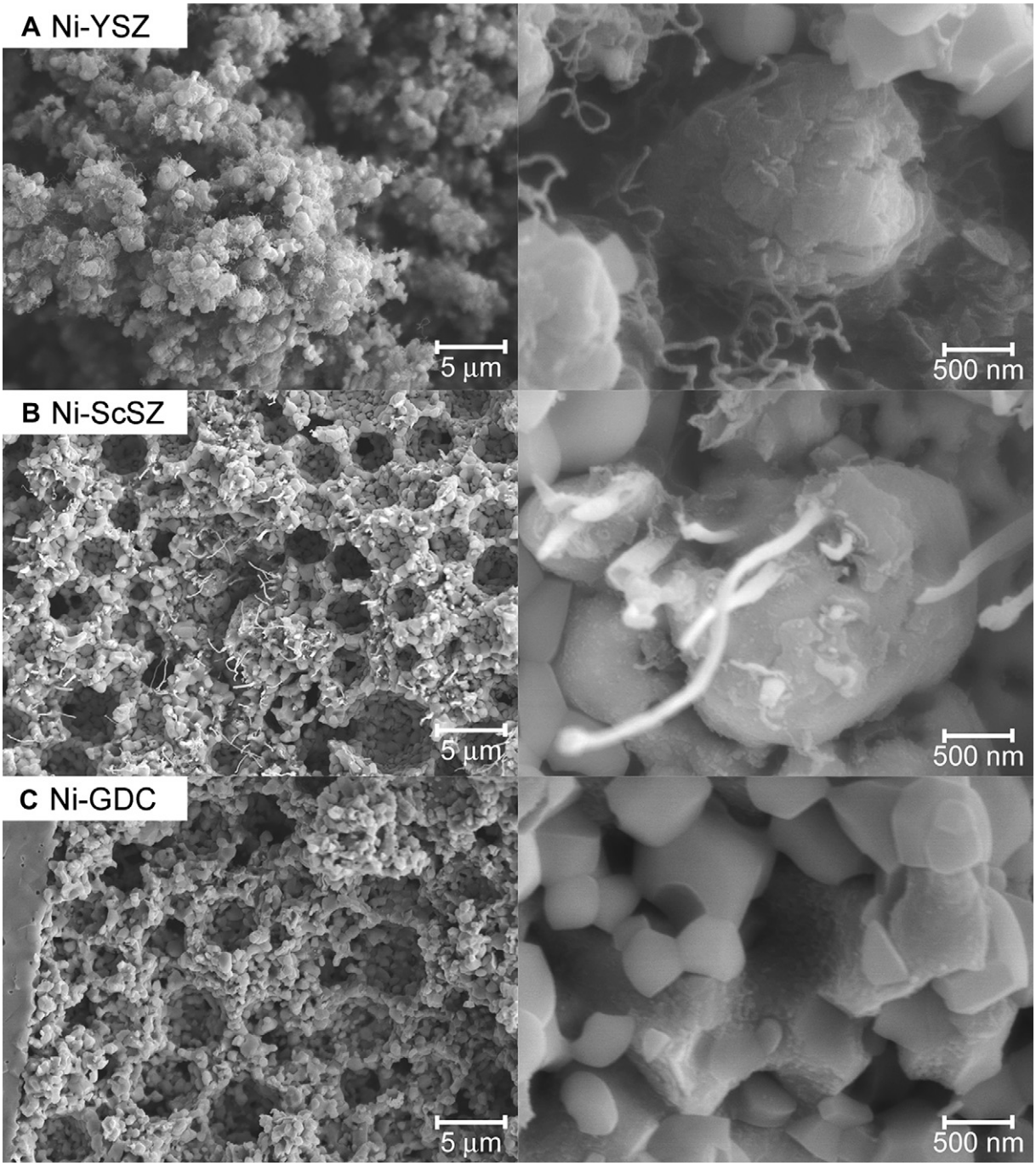


**Fig. 4.** Scanning electron images of Ni–YSZ (A), Ni–ScSZ (B) and Ni–GDC (C) anodes after direct butane power generation at 610 °C.

That is, the deposited carbon is oxidized by reaction (4), and the ceria is oxidized by water and carbon dioxide (reactions (5) and (6)), which are produced by the power generation. The weight increase rate became small for the Ni–GDC in humidified butane as shown in Fig. 1, due to the redox cycle of deposited carbon and ceria by the reactions (4) and (5). Furthermore, the ceria can be oxidized electrochemically by the following reaction, because ceria is a mixed $O^{2-}$ ionic/electronic conductor.

$$CeO_{2-n} + nO^{2-} \rightarrow CeO_2 + 2ne^- \quad (7)$$

The reforming of butane and the electrochemical oxidation of carbon also occurs by the production of water during the power generation (reactions (2) and (3)). We used the microstructural controlled anode with highly dispersed GDC powders several hundred nanometers in diameter prepared by co-precipitation method (Fig. 4C). This Ni–GDC anode resulted in the high durability during the butane direct power generation due to the promotion of ceria redox. In general, SOFCs are not operated under the carbon deposition condition. However, small-scale portable SOFCs are at risk of operation under non-humidified condition during emergencies as the control systems are simplified to reduce the costs. The portable power sources with high efficiency and durability is expected to be made possible by the use of the Ni–GDC anode-supported microtubular SOFCs developed in this study.

## 4. Conclusions

In this study, we demonstrated direct butane power generation for microtubular SOFCs with microstructural controlled Ni–YSZ, Ni–ScSZ and Ni–GDC composite anodes. The weight decrease of NiO–GDC was larger and faster than that of NiO–YSZ and NiO–ScSZ in hydrogen, which suggests that a part of ceria was also reduced from $Ce^{4+}$ to $Ce^{3+}$. The redox of ceria also contributed the suppression of carbon deposition on the Ni–GDC at 610 °C in humidified butane. The cells with the Ni–YSZ and Ni–ScSZ anodes deteriorated rapidly over a period of 3–4 h at 610 °C and a low S/C ratio of 0.044 in butane. Carbon was coated on Ni catalysts and carbon nanofibers were grown from the interface between Ni and oxide particles for the Ni–YSZ and Ni–ScSZ anodes after direct butane power generation. On the other hand, power can be generated continuously for more than 24 h at 610 °C and S/C = 0.044 in butane for the cell with the Ni–GDC anode. The microstructure of the Ni–GDC anode was kept and no carbon nanofiber was observed after direct butane power generation. We used the microstructural controlled anode with highly dispersed GDC powders several hundred nanometers in diameter, which resulted in the high durability during direct butane power generation.

## References

[1] K. Eguchi, H. Kojo, T. Takeguchi, R. Kikuchi, K. Sasaki, Solid State Ionics 152–153 (2002) 411–416.
[2] E.P. Murray, T. Tsai, S.A. Barnett, Nature 400 (1999) 649–651.
[3] H. Sumi, K. Ukai, Y. Mizutani, H. Mori, C.-J. Wen, H. Takahashi, O. Yamamoto, Solid State Ionics 174 (2004) 151–156.
[4] T. Iida, M. Kawano, T. Matsui, R. Kikuchi, K. Eguchi, J. Electrochem. Soc. 154 (2007) B234–B241.
[5] X. Wang, R.J. Gorte, Appl. Catal. A 224 (2002) 209–218.
[6] K. Yamaji, H. Kishimoto, Y. Xiong, T. Horita, N. Sakai, M.E. Brito, H. Yokokawa, Solid State Ionics 179 (2008) 1526–1530.
[7] H. Sumi, Y.-H. Lee, H. Muroyama, T. Matsui, K. Eguchi, J. Electrochem. Soc. 157 (2010) B1118–B1125.
[8] H. Sumi, P. Puenginda, H. Muroyama, T. Matsu, K. Eguchi, J. Power Sources 196 (2011) 6048–6054.
[9] D.L. Trimm, Catal. Today 37 (1997) 233–238.
[10] S.D. Park, J.M. Vohs, R.J. Gorte, Nature 404 (2000) 265–267.
[11] R.J. Gorte, H. Kim, J.M. Vohs, J. Power Sources 106 (2002) 10–15.
[12] S.I. Lee, J.M. Vohs, R.J. Gorte, J. Electrochem. Soc. 151 (2004) A1319–A1323.
[13] J.C. Ruiz-Morales, J. Canales-Vázquez, C. Savaniu, D. Marrero-López, W. Zhou, J.T.S. Irvine, Nature 439 (2006) 568–571.
[14] L. Sun, Y. Hao, C. Zhang, R. Ran, Z. Shao, Int. J. Hydrogen Energy 35 (2010) 7971–7981.
[15] M. Lo Faro, A. Stassi, V. Antonucci, V. Modafferi, P. Frontera, P. Antonucci, A.S. Aricò, Int. J. Hydrogen Energy 36 (2011) 9977–9986.
[16] S.A. Venâncio, P.E.V. de Miranda, Scr. Mater. 65 (2011) 1065–1068.
[17] X.-F. Ye, J. Zhou, S.R. Wang, F.R. Zeng, T.L. Wen, Z.L. Zhan, Int. J. Hydrogen Energy 37 (2012) 505–510.
[18] P.K. Cheekatamarla, C.M. Finnerty, J. Cai, Int. J. Hydrogen Energy 33 (2008) 1853–1858.
[19] T.H. Shin, S. Ida, T. Ishihara, J. Am. Chem. Soc. 133 (2011) 19399–19407.
[20] H. He, J.M. Vohs, R.J. Gorte, J. Electrochem. Soc. 154 (2007) B694–B699.
[21] M.D. Gross, J.M. Vohs, R.J. Gorte, J. Power Sources 144 (2005) 135–140.
[22] M. Horiuchi, F. Katagiri, J. Yoshitake, S. Suganuma, Y. Tokutake, H. Kronemayer, W.G. Bessler, J. Power Sources 189 (2009) 950–957.
[23] T. Kim, G. Liu, M. Boaro, S.-I. Lee, J.M. Vohs, R.J. Gorte, O.H. Al-Madhi, B.O. Dabnbousi, J. Power Sources 155 (2006) 231–238.
[24] H. Kishimoto, T. Horita, K. Yamaji, Y. Xiong, N. Sakai, H. Yokokawa, Solid State Ionics 175 (2004) 107–111.
[25] L.F.D. Camacho, J.A.M. Vivas, Fuel 88 (2009) 1970–1974.
[26] Y. Shiratori, T. Oshima, K. Sasaki, Int. J. Hydrogen Energy 33 (2008) 6316–6321.
[27] K. Kendall, M. Palin, J. Power Sources 71 (1998) 268–270.
[28] K. Kendall, C.M. Finnerty, G.A. Tompsett, P. Windibank, N. Coe, Electrochemistry 68 (2000) 403–406.
[29] K. Yashiro, N. Yamada, T. Kawada, J.O. Hong, A. Kaimai, Y. Nigara, J. Mizusaki, Electrochemistry 70 (2002) 958–960.
[30] T. Suzuki, Y. Funahashi, T. Yamaguchi, Y. Fujishiro, M. Awano, Electrochem. Solid-State Lett. 10 (2007) A177–A179.
[31] T. Suzuki, Z. Hasan, Y. Funahashi, T. Yamaguchi, Y. Fujishiro, M. Awano, Science 325 (2009) 852–855.
[32] H. Sumi, T. Yamaguchi, K. Hamamoto, T. Suzuki, Y. Fujishiro, T. Matsui, K. Eguchi, Electrochim. Acta 67 (2012) 159–166.
[33] Z.A. Quan, Y.N. Qin, C. Liu, Appl. Catal. 70 (1991) 1–8.
[34] S. McIntosh, J.M. Vohs, R.J. Gorte, J. Electrochem. Soc. 150 (2003) A470–A476.
[35] M.L. Toebes, J.H. Bitter, A. Jos van Dillen, K.P. de Jong, Catal. Today 76 (2002) 33–42.